ELSEVIER

Biophysical Chemistry 101–102 (2002) 333–345

Biophysical Chemistry

www.elsevier.com/locate/bpc

Effect of neutral lipids on coexisting phases in monolayers of pulmonary surfactant

Bohdana M. Discher[a,1], Kevin M. Maloney[b,2], David W. Grainger[c], Stephen B. Hall[a,d,e,*]

[a]*Department of Biochemistry and Molecular Biology, Oregon Health and Science University, Portland, OR 97201-3098, USA*
[b]*Department of Chemistry, Biochemistry and Molecular Biology, Oregon Graduate Institute of Science and Technology, Portland, OR 97006, USA*
[c]*Department of Chemistry, Colorado State University, Fort Collins, CO 80523-1872, USA*
[d]*Department of Medicine, Oregon Health & Science University, Portland, OR 97201-3098, USA*
[e]*Department of Physiology and Pharmacology, Oregon Health and Science University, Portland, OR 97201-3098, USA*

Abstract

We previously established that compression of monolayers containing the lipids in pulmonary surfactant, with or without the surfactant proteins, initially leads to phase separation. On further compression, however, phase coexistence terminates at a critical point that requires the presence of cholesterol. The studies reported here address the changes in the phospholipid phase diagram produced by cholesterol. We used the two systems of the lipids from calf surfactant with and without the surfactant proteins. For both systems, we began with the postulate that cholesterol had no effect on the composition of other constituents in the two phases, and then used the known behavior of interfacial tension at a critical point to test the two extreme cases in which the cholesterol partitions exclusively into condensed domains or into the surrounding film. Measurements of surface potential along with the fraction of the nonfluorescent area and the radius of the domains, both obtained by fluorescence microscopy, for films with and without cholesterol allowed calculation of the interfacial tension between the two phases. Only the model that assumes the presence of cholesterol within the domains accurately predicts a decreasing line tension during film compression toward the critical point. That model, however, also predicts an unlikely decrease during compression of the dipole moment density for the condensed phase. Our results are best explained in terms of cholesterol partitioning predominantly into the condensed domains, with a resulting partial redistribution of the phospholipids between the two phases.

Keywords: Phase separation; Dipalmitoyl phosphatidylcholine; Line tension; Surface potential; Cholesterol; Critical point

1. Introduction

Phase separation of phospholipids provides a mechanism by which both soluble and insoluble components may be compartmentalized in biological systems. Although this phenomenon is more widely recognized for cellular membranes [1], phase separation has also been considered important for organizing monomolecular films of pul-

*Corresponding author. Molecular Medicine, Mail Code NRC-3, Oregon Health & Science University, Portland, OR 97201-3098, USA. Tel.: +1-503-494-6667; fax: +1-503-494-7368.

E-mail address: sbh@ohsu.edu (S.B. Hall).

[1] Present address: Department of Biochemistry and Biophysics, University of Pennsylvania, 422 Curie Boulevard, Philadelphia, PA 19104-6059, USA.

[2] Present address: Charles River Laboratories, 57 Union Street, Worcester, MA 01608, USA.

0301-4622/02/$ - see front matter
PII: S0301-4622(02)00191-6

monary surfactant. These films are essential for stabilizing the alveolar air spaces of the lungs. A thin layer of liquid, either continuous or discontinuous [2], lines the alveoli, and the surface tension of the air/water interface produces an inward recoil that tends to collapse the lungs. To counteract that effect, the type II pneumocytes synthesize and secrete a mixture composed mostly of phospholipids with some cholesterol and specific proteins that together acts as a surfactant. After adsorbing to the air/water interface, the films of pulmonary surfactant tend to spread laterally, generating a two-dimensional surface pressure that lowers surface tension. During exhalation, the shrinking alveolar surface area compresses the interfacial films to surface pressures that are remarkably high and that persist in static lungs for remarkably prolonged durations [3,4]. The magnitude and persistence of these pressures requires the presence of a solid film. For fluid monolayers, a compressive transition in which constituents collapse from the two-dimensional surface to form a three-dimensional bulk phase limits surface pressure to a maximum equilibrium value (π_e). Prolonged elevation of surface pressures above π_e, such as observed in the lungs, indicates resistance to flow into the collapsed phase and hence a solid film.

The classical model of pulmonary surfactant assumes equilibrium phase behavior, and therefore concludes that the functional film must occur as the solid tilted-condensed (TC) phase [5]. Because only one of the multiple constituents in pulmonary surfactant, dipalmitoyl phosphatidylcholine (DPPC), forms the TC phase in single component films at physiological temperatures [6], the model also contends that the solid film is highly enriched in DPPC. The change in composition from the freshly synthesized mixture required by the model might occur by selective collapse of constituents other than DPPC when the compressed film first exceeds π_e [5,7,8]. Lateral phase separation, in which DPPC forms metastable TC domains while all other constituents are confined to a rapidly collapsing liquid-expanded (LE) phase, provides one mechanism by which selective exclusion of components other than DPPC could occur [5].

We have shown previously that compression of monolayers containing the complete set of constituents in extracted calf surfactant (calf lung surfactant extract, CLSE) initially induces phase separation [9]. Fluorescence microscopy and Brewster angle microscopy both detect the formation of discrete domains. In experiments with the subfraction of calf surfactant that contains only the complete set of purified phospholipids (PPL), but not the proteins or cholesterol, measurements on the area of each phase and their response to DPPC added to the film allowed construction of a phase diagram. This analysis indicates that the domains contain essentially pure DPPC [10]. If the fluid LE phase in these mixed films would collapse from the interface much faster than the solid TC domains, then the phase separation would provide the basis for enriching the film's content of DPPC.

Although these initial results with CLSE and PPL fit with the selective exclusion model based on phase separation, subsequent findings do not. With further compression of surfactant-related films that include cholesterol, phase separation terminates [9,11]. Immediately following a shape transition in which the circular condensed domains suddenly adopt highly irregular contours, the interface between the two phases vanishes, reestablishing a homogeneous film. This behavior is characteristic of a critical point in the phase diagram. Interfacial tension, termed 'line tension' in the two-dimensional monolayer, approaches zero when the two phases become increasingly similar near a critical point, allowing extension of the boundary between the two phases just prior to remixing. The termination of phase separation at surface pressures below π_e eliminates the basis for selective exclusion of compounds other than DPPC, and provides one further element in a mounting body of evidence which argues that surfactant function is not as firmly based on phase behavior as previously thought [12,13].

The critical behavior in surfactant films requires the presence of cholesterol [11]. Phase coexistence persists to π_e if cholesterol is removed from the surfactant phospholipids, and adding it back restores remixing. Pulmonary surfactant then represents one of several systems containing cholesterol and phospholipids that have recently been

shown to exhibit critical behavior [14–16]. The studies reported here address the question of how cholesterol changes the two phases in cholesterol–phospholipid mixtures, using pulmonary surfactant as one example of such a system that is directly relevant to monolayers in the lungs.

2. Materials, methods and theory

2.1. Materials

Extracted calf surfactant (CLSE), prepared according to established procedures [17], was fractionated to exclude specific components using column chromatography by a slight modification of a previously published protocol [18]. Gel permeation chromatography separates the proteins, phospholipids, and neutral lipids into separate peaks [19]. Pooling selected fractions provides preparations that contain the PPL, the neutral and phospholipids (N&PL), and the surfactant proteins and phospholipids (SP&PL) [18]. Each of these preparations then contains the complete set of surfactant phospholipids with or without the surfactant proteins and neutral lipids. Although the protein and phospholipid peaks overlapped in the original protocol [18], a longer column achieved complete separation on a single pass for the materials studied here. Preparations were eluted from LH-20 matrix (LKB-Pharmacia, NJ) with a solvent of acidified chloroform–methanol (0.1 N $HCl:CHCl_3:CH_3OH$; 2:19:19 v:v:v) [19,20], followed by extraction of the constituents into chloroform [21]. Samples of SP&PL suffered variable losses of proteins and were supplemented with protein purified separately to obtain the protein/phospholipid ratio found for CLSE [18]. The ratio of cholesterol to phospholipids (μmol:μmol) varied from 0.053 to 0.074 for CLSE and from 0.045 to 0.071 for N&PL.

DPPC was obtained from Avanti Polar Lipids, Inc. (Alabaster, AL) and used without further analysis or purification. *N*-(Lissamine rhodamine B sulfonyl)-1,2-dihexadecanoyl-sn-glycero-3-phosphoethanolamine (rhodamine-DPPE) was purchased from Molecular Probes (Eugene, OR).

Reverse-osmosis grade water for these studies was obtained from purification systems purchased either from Millipore (Bedford, MA) or Barnstead (Dubuque, IA) and had resistivity of approximately 18 MΩ cm. All glassware was acid-cleaned. All solvents were at least reagent-grade and contained no surface active stabilizing agents.

2.2. Methods

2.2.1. Biochemical assays

Phospholipid concentrations were determined by measuring the phosphate content [22] of measured aliquots. Protein was assayed by amido black staining of trichloroacetic acid-precipitable material [23], with bovine serum albumin as a standard. Cholesterol (free and esterified) was measured by reduction with ferrous sulfate [24].

2.2.2. Isotherms

The variation of surface pressure and surface potential with area were measured on a commercially available Langmuir trough (KSV-3000, KSV Instruments, Helsinki, Finland). Monolayers were spread by depositing aliquots of chloroform solutions on a subphase of 10 mM Hepes pH 7.0, 150 mM NaCl, and 1.5 mM $CaCl_2$ (HSC), followed by a 10-min interval to allow for evaporation of the chloroform. Surface pressure and surface potential were recorded simultaneously during compression at 2.8 $Å^2$/(phospholipid molecule·min) and 20 °C. Surface pressure (π) was measured using a Wilhelmy plate. Molecular areas ($\bar{A}$) were expressed in terms only of phospholipid for reasons of simplicity and accuracy, with no attempt to correct for the presence of neutral lipid and protein molecules. $\pi - \bar{A}$ curves were reproducible between experiments to within 2 $Å^2$/(phospholipid molecule) and 0.4 mN/m. Surface potential was measured with an ionizing electrode. The electrode, which contains ^{241}Am as a source of α particles to provide a conducting circuit, was placed 1–2 mm above the subphase. If the potential difference, measured by a pH meter with a high impedance amplifier, between this electrode and a reference electrode in the subphase is offset to zero for a clean air/water interface, then the

measured voltage, ΔV, with a surface film provides the difference in surface potential for the interface with and without the film [25].

2.2.3. Fluorescence microscopy

Epifluorescence microscopy used a Zeiss-ACM microscope [26] with a 50× objective to visualize lipid monolayers [27–29] on the surface of a custom-built Langmuir trough. The Teflon trough had a surface area of 108 cm^2 and subphase volume of 100 ml [30], the temperature of which was regulated to ± 1 °C with water pumped through jackets surrounding the trough. Samples of surfactant preparations containing 1% (mol/mol phospholipid) of rhodamine-DPPE were spread in approximately 80 μl of chloroform on a subphase containing HSC to give an initial molecular area of 150 $Å^2$/(phospholipid molecule). Films were then compressed at 2.8 $Å^2$/(phospholipid molecule min) to specific surface pressures at which images were recorded on the static film. A Hamamatsu C2400 SIT camera recorded fluorescence images either to VHS video tape for later analysis or directly to computer (Quadra 650, Apple, Inc., Cupertino, CA with LG-3 frame grabber, Scion Corp, Frederick, MD). A C-shaped Teflon mask placed directly in the trough and extending through the interface minimized movement of the monolayer [26,31]. Images obtained inside and outside the mask at frequent intervals ensured that the mask created no artifacts. The high contrast between the fluorescent and nonfluorescent regions of the film allowed counting of pixels above and below a threshold grayscale to provide the area of each phase.

2.3. Theory

Our analysis ultimately requires values of the line tension, λ, between the two phases within the monolayer. For a monolayer at strict equilibrium, the discontinuous phase occurs as circular domains, the radius of which, R, is determined by λ and $\Delta\mu$, the difference in dipole densities between the two phases [32]. We therefore have derived expressions for $\Delta\mu$ in terms of measurable quantities, and for λ in terms of R and $\Delta\mu$.

2.3.1. Dipole moment densities

When a film separates into condensed and expanded phases, the component of the dipole moments normal to the interface for molecules in the two phases, m_c and m_e, and the average normal component of dipole moments for the total film, m, are related by:

$$m = f_c m_c + f_e m_e, \tag{1}$$

where f_c and f_e are the fractions of total molecules within the film that are located in each phase. The dipole moment density, μ_x, for these normal components is then given by

$$\mu_x = \frac{m_x}{\bar{A}_x} \tag{2}$$

where $\bar{A}$ is molecular area and x refers to the particular phase or to the average film. The fraction of molecules in each phase, f_x, is related to its experimentally accessible fractional area, ϕ_x, according to

$$f_x \bar{A}_x = \phi_x \bar{A} \tag{3}$$

Because

$$\phi_c + \phi_e = 1 \tag{4}$$

substitution of Eqs. (2)–(4) into Eq. (1) yields an expression for the average dipole moment density, μ, in terms of the values μ_c and μ_e for each phase, and the fraction of the interfacial area, ϕ_c, occupied by the condensed phase:

$$\mu = \mu_c \phi_c + \mu_e (1 - \phi_c) \tag{5}$$

The average dipole moment density for the film, μ, is related to the surface potential, ΔV, by the Helmholtz equation,

$$\mu = \varepsilon_0 \Delta V \tag{6}$$

where ε_0 is the permittivity of vacuum ($\varepsilon_0 = 8.854 \times 10^{-12}$ $C^2/N/m^2$).

Given the fraction of the interface occupied by the condensed phase and the dipole moment density of one phase, Eqs. (5) and (6) can be used to calculate the dipole moment density of the other phase from measurements of the surface potential ΔV:

$$\mu_e = \frac{\varepsilon_0 \Delta V - \phi_c \mu_c}{1 - \phi_c} \tag{7}$$

$$\mu_c = \frac{\varepsilon_0 \Delta V - \mu_e(1-\phi_c)}{\phi_c} \quad (8)$$

2.3.2. Line tension

The balance between the line tension, λ, and the difference in dipole moment density, Δμ, determines the equilibrium radius, *R*, of the domains [32]. Consequently, line tension can be determined from *R* and Δμ. Relationships between λ, Δμ and *R* have been derived previously, but only in terms of 'ansatz' equations [33]. The experiments here require an exact expression. The general approach is to express the energy for a condensed phase with fixed total area distributed among domains with uniform but variable radii. Minimization of the system energy then provides an expression relating λ, Δμ and *R* at equilibrium. The free energy of the system consists of the electrostatic energy, E_{el}, which results from dipolar repulsions, and the line tension energy, E_λ. Under the assumption that the dipoles do not rotate with respect to each other, the electrostatic energy for two normal components of dipole moments inside the domain, m_c and m_c', is

$$E_{el}(m,m') = \frac{m_c m'_c}{4\pi\varepsilon_0 |r-r'|^3} \quad (9)$$

where $|r-r'|$ is the distance between the dipoles [34]. Since the distribution of the condensed phase into multiple domains does not affect the energy of the expanded phase, the dipole moment density μ_e does not contribute to the free-energy change. Therefore we can consider μ_e to be 'background' dipole moment density and subtract it from the dipole moment densities of both phases [32]. Then $\mu_e = 0$, and the difference in dipole moment densities between the two phases, $\Delta\mu \equiv \mu_c - \mu_e = \mu_c$, requires determination only of the value for the condensed domains.

From Eq. (2) then

$$E_{el}(m,m') = \frac{(\Delta\mu)^2}{4\pi\varepsilon_0 |r-r'|^3} \bar{A}_c \bar{A}'_c \quad (10)$$

To obtain the electrostatic energy of a complete domain, E_{el}(domain), we must integrate over all pairs of area elements within the domains:

$$E_{el}(\text{domain}) = \frac{1}{2}\frac{1}{4\pi\varepsilon_0}(\Delta\mu)^2 \int\int |r-r'|^{-3} d\bar{A}_c d\bar{A}'_c \quad (11)$$

The factor of $\frac{1}{2}$ comes from a double counting of pairs of elements in the integrand. The energy of each circular domain contributed by line tension is $E_\lambda = 2\pi R\lambda$, where *R* and λ are the equilibrium radius of the domain and the line tension, respectively. The derivation of the line tension from minimization of the total energy $E = E_{el} + E_\lambda$ then proceeds as published previously [32]. When the energy of the system is at a minimum,

$$R_{eq} = \frac{e^3\delta}{4} e^{(4\pi\varepsilon_0\lambda/\Delta\mu^2)} \quad (12)$$

and therefore

$$\lambda = \frac{\Delta\mu^2}{4\pi\varepsilon_0} \ln\left(\frac{4R_{eq}}{e^3\delta}\right) \quad (13)$$

where *e* is the base of the Naperian logarithm, and δ is an effective distance between neighboring dipoles at the interface, taken as roughly 10 Å [35]. Estimates of R_{eq} by fluorescence microscopy and of Δμ from measurements of surface potential then provide the basis for calculating λ.

3. Results

We considered the behavior of two films derived from pulmonary surfactant, both of which contain cholesterol. Extracted calf surfactant (CLSE) contains the complete set of hydrophobic constituents, which are the components responsible for surface activity. Removal of the surfactant proteins yields a preparation containing only the N&PL [18]. For both CLSE and N&PL, the corresponding preparation that lacks cholesterol is also available for comparison. Removal of cholesterol from CLSE yields the SP&PL, and the same process for N&PL produces the PPL [18]. Fluorescence microscopy detected initial phase separation in films containing each of these preparations (Fig. 1), but the shape transition and remixing that indicates critical behavior occurred only for CLSE and N&PL [11].

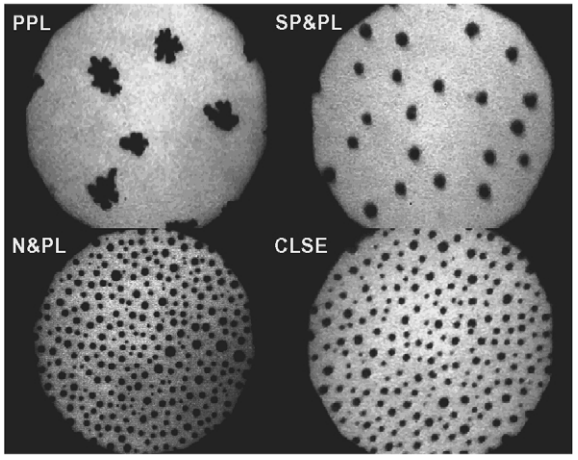

Fig. 1. Coexisting phases in surfactant-related monolayers during lateral compression. Films containing the different preparations derived from calf surfactant were mixed with 1% (mol:mol phospholipid) rhodamine-DPPE and spread on the surface of a Langmuir trough. Films were compressed at 2.8 $Å^2$/(phospholipid molecule·min) and 20 °C to 10 mN/m, and then to higher surface pressures at 5 mN/m increments after obtaining microscopic images on the static film. Images here were obtained at 20 mN/m. Diameter of the visual field is 300 μm. Previously published micrographs at these and other surface pressures show that the shapes of the nonfluorescent domains changes little for any given film with time, but that the irregular forms for PPL relax to circular shapes over a period of hours [9,11].

Our studies were designed to determine how the phase diagram of the surfactant phospholipids could change with the additional presence of cholesterol to generate a critical point. To establish the location of cholesterol, we assumed as a first approximation that the nonfluorescent domains in films with and without cholesterol differed only in their content of that compound, and similarly for the fluorescent regions. The composition of phospholipids in each phase would be unaffected by the added cholesterol. We then postulated two extreme cases in which cholesterol resided either completely within the condensed domains or entirely in the surrounding film. The known behavior of line tension at a critical point, where interfacial tension must cease to exist, provided a test of each model.

For a monolayer at strict equilibrium, the discontinuous phase would occur as circular domains, the radius of which, R, can be expressed in terms of λ, the line tension, and $\Delta\mu$, the difference in dipole moment density between the two phases (Eq. (13)) [32]. We used this relationship to calculate λ from measured values of R and $\Delta\mu$. Fluorescence micrographs provided values of R. Surface potential provided μ_x for the phase containing no cholesterol according to the model. The relative areas of each phase, determined microscopically, the average μ for the film, and μ_x for one phase were then used to calculate μ_y for the other phase according to each model (Eqs. (7) and (8)) and then $\Delta\mu$. The variation of λ during compression could therefore be established for two films—the surfactant lipids with and without the proteins—and used to test the different models of cholesterol's location.

Our analysis required values for R, the radius of the circular nonfluorescent domains at equilibrium. Fluorescence micrographs showed that the domains in films containing protein or cholesterol were roughly circular throughout compression except immediately prior to remixing. We assumed that these represented roughly equilibrium forms. For PPL, the initial shape of the condensed domains deviated far from circles (Fig. 1) [10,11,13]. We have shown previously, however, that these irregular shapes represent nonequilibrium forms that relax to circles over periods of hours [11]. The area of the condensed phase changed less than 5% during relaxation. The initial area therefore approximated the equilibrium area, and could be used to calculate the necessary equilibrium value of R. For SP&PL, N&PL and CLSE, the circular domains varied somewhat in size within any micrograph. We have previously determined the fraction of the area covered by the nonfluorescent phase, ϕ_c, as well as the density of the domains, ρ, in terms of number per area [9,11]. These data allowed us to calculate the average radius R of the circular domains:

$$R = \sqrt{\frac{\phi_c}{\pi\rho}} \tag{14}$$

Because of the small change in area between the initial and circular domains for PPL, the same expression was used to calculate an approximate

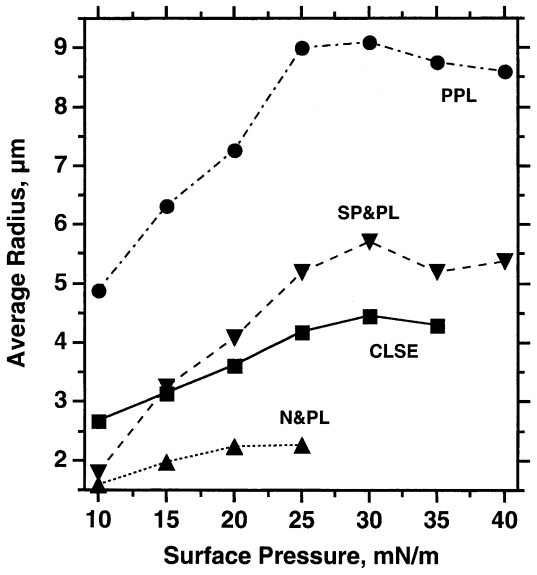

Fig. 2. Size of condensed domains at different surface pressures. Fluorescent micrographs such as those in Fig. 1 provided the average radius, obtained from the total nonfluorescent area and the number of domains. Data for CLSE and N&PL do not extend above 35 and 25 mN/m, respectively, because phase separation terminates above those surface pressures.

equilibrium radius for those films as well. These average radii (Fig. 2) were then used in the calculations of line tension.

Measurements of surface potential provided values of $\Delta\mu$. At all surface pressures, surface potential varied smoothly without large fluctuations. This behavior indicated that the tip of the electrode was sufficiently larger than the individual domains that the measurements provide the average potential for the film representing the weighted contributions of the two phases. The average dipole moment density was then calculated according to the Helmholtz equation (Eq. (6)). Surface potential for CLSE deviated substantially from values for DPPC, particularly at molecular areas less than roughly 70 Å^2/molecule, approximately half-way across the coexistence plateau in the surface pressure–area isotherm for DPPC, where the slope of the surface potential isotherm for DPPC increased abruptly (Fig. 3). PPL, N&PL and SP&PL all had surface potentials quite similar to values for CLSE, and the effect of removing the proteins and/or neutral lipids on the average dipole moment density was small (Fig. 3).

Surface potential directly yields only the average dipole moment density. The values of $\Delta\mu$, required to calculate line tension, can be obtained from the average dipole density if the fraction of surface area occupied by each phase and the dipole moment for one phase are known (Eqs. (7) and (8)). The fluorescence micrographs provided the fractional areas. The dipole moment density for one of the two phases followed from previously published findings concerning the composition of the domains and from the two models of the cholesterol distribution.

We have previously shown that the domains in PPL contain essentially pure DPPC [10]. The dipole moment density should therefore be the same as for TC DPPC, which can be calculated from the measured surface potential for DPPC monolayers at all surface pressures above the coexistence region:

$$\mu_c = \mu_{DPPC} = \varepsilon_0 \Delta V_{DPPC} \quad (15)$$

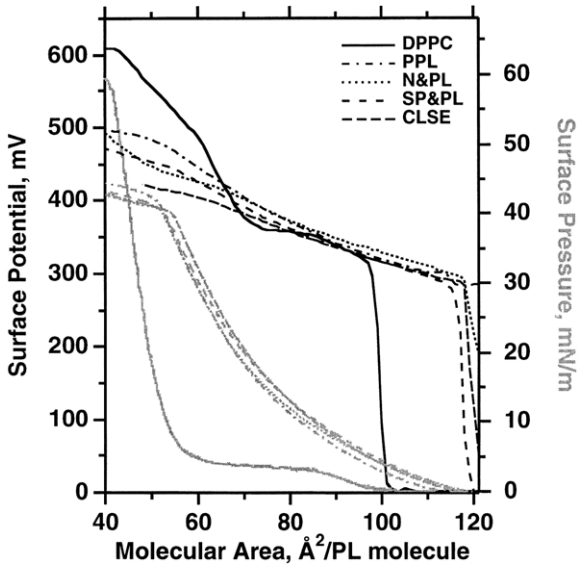

Fig. 3. Isotherms for monolayers containing surfactant-related preparations. Surface potential (black curves, left axis) and surface pressure (gray curves, right axis) were measured during compression of the surface area at 2.8 Å^2/(phospholipid molecule·min) and 20 °C for each of the different preparations derived from calf surfactant.

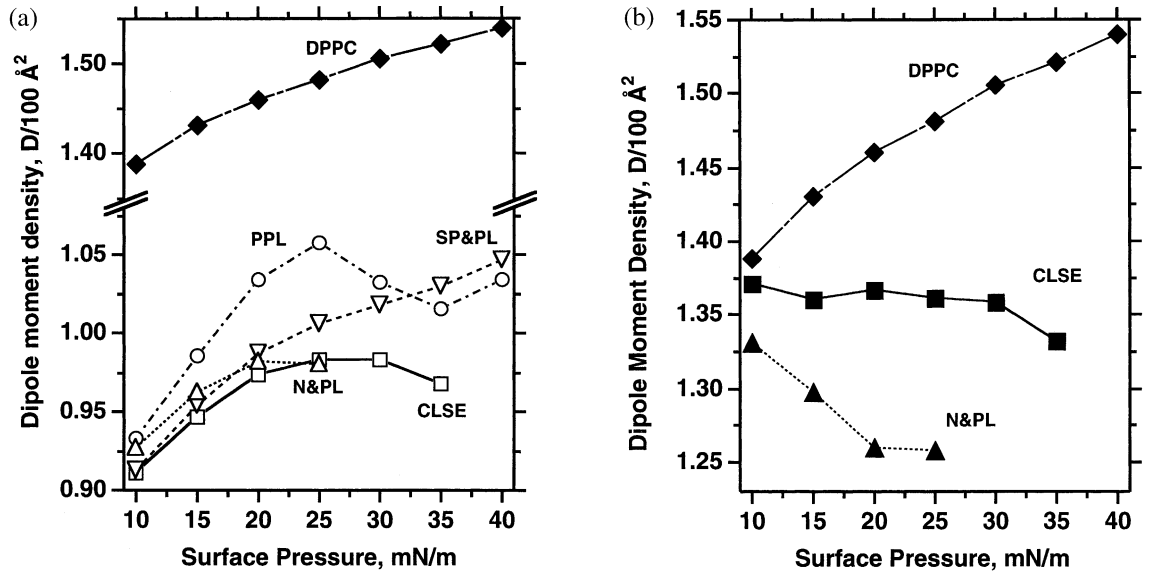

Fig. 4. Dipole moment density for cholesterol located exclusively inside or outside of the condensed domains. Filled symbols give values for condensed domains, and open symbols represent the surrounding film. (a) Values if domains contain no cholesterol. Filled symbols give values for condensed domains, obtained from surface potentials measured on DPPC at surface pressures above the coexistence region where the film is homogeneously TC. Domains in all of the mixed films would also contain only DPPC, and therefore would have the same values. Open symbols give values calculated for the expanded phase based on the surface potentials measured for the films, fractional areas of the phases obtained by fluorescence microscopy, and the assumed dipole moment density of DPPC for the condensed domains. (b) Values if domains contain all of the cholesterol. The surrounding LE phase for N&PL and CLSE would then have the same composition as PPL and SP&PL, respectively, and the dipole moment density would be given by the appropriate open symbols in (a). The filled symbols here give calculated values for the condensed domains based on the surface potentials measured for the films, the fractional area obtained by fluorescence microscopy, and the assumed dipole moment density from (a).

In SP&PL, which differs from PPL only by the additional presence of the surfactant proteins, the domains probably have the same composition. In studies with a simple mixture chosen to replicate pulmonary surfactant, both proteins remained outside the domains [36]. We therefore assumed that for both PPL and SP&PL, the dipole moment density of the domains could be obtained from measurements on DPPC. Values for the expanded phase could then be calculated from fractional areas for the two phases and the surface potentials for the films.

The compositions of CLSE and N&PL differ from those of SP&PL and PPL, respectively, only by the additional presence of cholesterol. Our analysis assumes that the compositions of the two phases were unaffected by cholesterol except for the content of that compound. For the two models of cholesterol distribution, the dipole moment density in the phase containing no cholesterol was therefore obtained from values for SP&PL or PPL. Values for the other phase could then be calculated from the measured surface potentials and fractional areas. For the model in which the domains contained no cholesterol, the dipole moment densities were similar for both the condensed and expanded phases in the four different films (Fig. 4a). The domains in all cases, whether according to prior reports or by constraint of the model, contained only DPPC, and so share that common dipole density. Values calculated for the surrounding expanded phase were also similar among the different preparations (Fig. 4a).

For the alternative model in which the domains instead contain all of the cholesterol, then the expanded phase would have the same μ_e as in

films of PPL and SP&PL (Fig. 4b). These values differed little from the dipole moment densities obtained according to the first model for the expanded phase in CLSE and N&PL (Fig. 4b). The μ_c calculated for the domains in CLSE and N&PL, however, decreased during compression and were distinctly lower than the values common to PPL, SP&PL and DPPC (Fig. 4b). Therefore the additional presence of cholesterol in surfactant-related monolayers produced opposite changes in μ_c and $\Delta\mu$ depending on which phase contained the cholesterol. Location of cholesterol in the condensed domains required values of μ_c and $\Delta\mu$ that decreased during compression. For cholesterol confined to the surrounding film, both μ_c and $\Delta\mu$ increased.

Line tension could then be calculated from the different values of $\Delta\mu$ and R according to Eq. (13). Compression produced an increase in line tension for all films in which the domains contained no cholesterol (Fig. 5). Line tension grew for PPL and for SP&PL, the preparations that contain no cholesterol, and for N&PL and CLSE considered according to the first model in which cholesterol resides only in the expanded phase. For the second model, however, in which the cholesterol partitions into the domains, line tension fell at higher surface pressures. Line tension decreased from 0.09 to 0.02 pN between 10 and 25 mN/m for N&PL, and from 0.13 to 0.06 pN between 10 and 35 mN/m for CLSE (Fig. 5). Line tensions that fall to low values, which are expected approaching a critical point, were predicted only by the model in which the cholesterol resided exclusively within the domains.

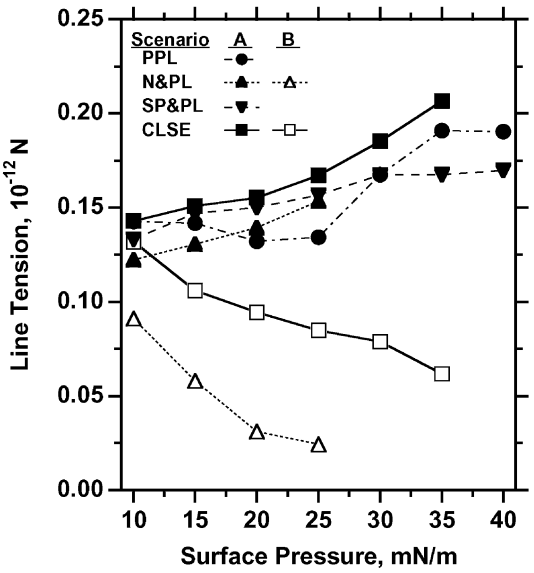

Fig. 5. Variation of line tension for each model of cholesterol distribution. Line tensions were calculated from the measured average radius for the domains and from the difference in dipole moment density calculated for each model. Calculations for filled symbols (Scenario A) assumed that the domains contained no cholesterol, and for the open symbols (Scenario B) that the domains contained all of the cholesterol.

4. Discussion

Our studies consider the manner in which cholesterol alters the behavior of the surfactant phospholipids in generating a critical point in the phase diagram. Our analysis assumes that the dark and bright phases in the films without cholesterol are each directly related to the corresponding phase when that compound is present. We then consider our experimental data in terms of the two extreme models in which cholesterol partitions exclusively into one phase or the other. Only the model in which cholesterol localizes to the condensed domains successfully predicts a line tension that decreases during compression toward the critical point. To the extent that the assumptions underlying the analysis are valid, these results suggest that the domains contain at least the preponderance of the film's cholesterol.

Our calculations have achieved a number of successes. The line tensions are consistent with values calculated or determined previously. Line tensions determined in other systems vary from 0.1 to 2 pN for films with a TC–LE interface [37,38], with a higher value of 5 pN found for solid–LE phase coexistence [39]. These values were obtained in systems that do not reach a critical point. The calculated line tensions in the surfactant preparations are at the lower end of the values reported by others as expected for films

that approach a critical point. Line tension has been determined previously for one other system with critical behavior. For the binary mixture of 30% cholesterol/70% dimyristoyl phosphatidylcholine, line tension decreases from 1.75 pN to zero during compression from 0 to 10 mN/m [35]. The actual values cannot be compared directly because our data are at surface pressures above 10 mN/m, but the previously reported line tensions agree in general with the values calculated here.

Our line tensions are also consistent with our own previously observed results. The calculations for both PPL and SP&PL, which lack cholesterol and therefore involve the least degree of uncertainty, indicate that line tension grows during compression. These results accurately predict the persistence of phase coexistence and the absence of a critical point observed for those preparations [11]. The calculations also correctly indicate the effect of the surfactant proteins in the films that do contain cholesterol. The fall in line tension is deferred to higher surface pressures for CLSE, which contains the proteins, relative to N&PL with only the lipids, in agreement with the observed result that remixing occurs at a higher surface pressure for CLSE than for N&PL [11]. Our results are internally consistent to this extent as well as in general agreement with previously published results.

The calculations, however, also predict behavior that seems unlikely. Segregation of cholesterol into the condensed domains, which produces the correct behavior of line tension, requires that the dipole moment density in the domains decreases during compression (Fig. 4B). This result would be somewhat surprising. Compression of phospholipid monolayers generally produces little change in the surface dipole moment, and therefore the dipole moment density should increase because of the smaller molecular area [40]. This general relationship is best established for the LE phase [41], but measurements with DPPC confirm that compression also increases the dipole moment density for the TC phase [42]. The limited data of which we are aware concerning the surface potential of cholesterol–phospholipid monolayers, although complicated by an unusual experimental design,[3] suggest similar behavior [43]. The predicted decrease in dipole moment density for the condensed phase during compression therefore suggests that the model in which cholesterol partitions exclusively into the domains, and otherwise leaves the compositions of the two phases unaltered, is not strictly correct.

Our analysis makes two assumptions of unproven validity. The first is that the measurements are made under conditions of strict equilibrium. The calculation of line tension assumes equilibrium where the energy of the system is at a minimum. Two components of the film's total energy, line tension and electrostatic energy, originate from phase separation [32]. The balance between these two factors determines the size of the individual domains. The energy of line tension, which is proportional to the length of the total interface, achieves a minimum when domains are large. In contrast, electrostatic energy is least when the domains are small (Eq. (11)). The separation of the condensed phase into more numerous domains increases the distance between their dipole moments when averaged across the entire film, resulting in lower electrostatic repulsion [32]. The calculations require that the estimates of R and $\Delta\mu$ accurately reflect equilibrium values. Although the assumption is probably not strictly true, the trends that occur with composition and with surface pressure seem likely to be qualitatively correct. This potential source of error therefore seems unlikely to produce erroneous conclusions of the qualitative sort emphasized here.

The second assumption is that the bright and dark phases each differ between films with and without cholesterol only in their content of that compound, and specifically that the presence of cholesterol has no effect on the composition of

[3] The cited measurements used a commercially produced vibrating plate 'Kelvin S' probe that yielded surface potentials with simple phospholipid monolayers roughly equivalent in absolute value to prior reports, but opposite in sign [44]. The difference from results with conventional methods has been explained in terms of the reference point, or ground, moving to the opposite side of the monolayer, from the air to the subphase [45,46]. We presume, therefore, that the results for the cholesterol–phospholipid monolayers are correct in magnitude but opposite in sign.

phospholipids in each phase. This seems more questionable, particularly in light of the decreasing dipole moment density predicted during compression for the condensed phase. A repartitioning of the phospholipids in response to cholesterol would fit better with our data. If the condensed domains contained unsaturated phospholipids as well as DPPC, the molecular area would be larger and the dipole moment density smaller than the values used here for μ_c, which were obtained from measurements on pure DPPC. The values of μ_e, calculated from the measured average dipole moment density, would then be larger. $\Delta\mu$, which must decrease during compression towards a critical point, could fall because of the decreasing gap between μ_c and μ_e, each of which individually continued to grow. A repartitioning of the phospholipids also agrees with behavior required by the critical point. In the phase diagram, the composition of the phase outside the coexistence region must change continuously, and so the compositions of the coexisting phases, including of the phospholipids, when compressed toward the critical point must become increasingly similar. A redistribution of the phospholipids between the two phases in response to added cholesterol therefore agrees with behavior expected at a critical point as well as providing a better explanation of our experimental results.

This tentative conclusion suggests an additional role for cholesterol in organizing biological systems. Recent evidence indicates that in biological mixtures of phospholipids, cholesterol can produce phase separation under conditions where none exists in its absence [47]. The role of phase separation in organizing components into distinct cellular compartments, for instance, is receiving increased acceptance [1]. Our results raise the possibility that for phospholipid mixtures that do form distinct phases on their own, cholesterol can modulate their contents. Variation of cholesterol levels could then provide an additional mechanism by which biological systems can control the sorting of constituents between different compartments.

In summary, we have used pulmonary surfactant as an example of a biologically relevant phospholipid mixture to determine the effect of cholesterol on separated phases. We have estimated line tension between the separated phases for simple postulated distributions of components to test which model best fits with behavior required at the critical point produced by the addition of cholesterol. Calculations accurately predict that subfractions of pulmonary surfactant which lack the neutral lipids should maintain non-zero line tension and retain immiscible phases. For the subfractions containing cholesterol, the model in which the domains contain all of the cholesterol accurately predicts decreasing line tension during compression towards the critical point established previously by fluorescence microscopy. That same model, however, also indicates an unlikely decrease in the dipole moment density of the condensed domains. More complicated behavior, in which cholesterol, predominantly located in the condensed domains, allows accommodation of some fraction of the phospholipids other than DPPC, therefore seems more likely.

Acknowledgments

Drs Edmund Egan of ONY, Inc. and Robert Notter of the University of Rochester provided CLSE. These studies were supported by funds from the National Institutes of Health (HL 03502 and 60914, SH), the National Science Foundation (NSF DMR 9596023, DG), the Whitaker Foundation (SH and DG), a 3M faculty fellowship (DG), the American Lung Association of Oregon (SH and DG), and a Tartar Trust fellowship (BMD). BMD gratefully acknowledges helpful discussions with Dr Dennis E. Discher, University of Pennsylvania. SH thanks John A. Schellman for the standard, however unattainable, of science done well.

References

[1] D.A. Brown, E. London, Structure and function of sphingolipid- and cholesterol-rich membrane rafts, J. Biol. Chem. 275 (2000) 17221–17224.

[2] K.L. Dorrington, J.D. Young, Development of the concept of a liquid pulmonary alveolar lining layer, Br. J. Anaesth. 86 (2001) 614–617.

[3] T. Horie, J. Hildebrandt, Dynamic compliance, limit cycles, and static equilibria of excised cat lung, J. Appl. Physiol. 31 (1971) 423–430.

[4] S. Schürch, Surface tension at low lung volumes: dependence on time and alveolar size, Respir. Physiol. 48 (1982) 339–355.
[5] A.D. Bangham, C.J. Morley, M.C. Phillips, The physical properties of an effective lung surfactant, Biochim. Biophys. Acta 573 (1979) 552–556.
[6] M.C. Kahn, G.J. Anderson, W.R. Anyan, S.B. Hall, Phosphatidylcholine molecular-species of calf lung surfactant, Am. J. Physiol.-Lung Cell. Mol. Physiol. 13 (1995) L567–L573.
[7] J.A. Clements, Functions of the alveolar lining, Am. Rev. Respir. Dis. 115 (6 part 2) (1977) 67–71.
[8] J.C. Watkins, The surface properties of pure phospholipids in relation to those of lung extracts, Biochim. Biophys. Acta 152 (1968) 293–306.
[9] B.M. Discher, K.M. Maloney, W.R. Schief, D.W. Grainger, V. Vogel, S.B. Hall, Lateral separation of interfacial domains in films of pulmonary surfactant, Biophys. J. 71 (1996) 2583–2590.
[10] B.M. Discher, W.R. Schief, V. Vogel, S.B. Hall, Phase separation in monolayers of pulmonary surfactant phospholipids at the air–water interface: composition and structure, Biophys. J. 77 (1999) 2051–2061.
[11] B.M. Discher, K.M. Maloney, D.W. Grainger, C.A. Sousa, S.B. Hall, Neutral lipids induce critical behavior in interfacial monolayers of pulmonary surfactant, Biochemistry 38 (1999) 374–383.
[12] J.M. Crane, S.B. Hall, Rapid compression transforms interfacial monolayers of pulmonary surfactant, Biophys. J. 80 (2001) 1863–1872.
[13] B. Piknova, W.R. Schief, V. Vogel, B.M. Discher, S.B. Hall, Discrepancy between phase behavior of lung surfactant phospholipids and the classical model of surfactant function, Biophys. J. 81 (2001) 2172–2180.
[14] J.P. Hagen, H.M. McConnell, Critical pressures in multicomponent lipid monolayers, Biochim. Biophys. Acta 1280 (1996) 169–172.
[15] S.L. Keller, W.H. Pitcher, W.H. Huestis, H.M. McConnell, Red blood cell lipids form immiscible liquids, Phys. Rev. Lett. 81 (1998) 5019–5022.
[16] S.L. Keller, T.G. Anderson, H.M. McConnell, Miscibility critical pressures in monolayers of ternary lipid mixtures, Biophys. J. 79 (2000) 2033–2042.
[17] R.H. Notter, J.N. Finkelstein, R.D. Taubold, Comparative adsorption of natural lung surfactant, extracted phospholipids, and artificial phospholipid mixtures to the air–water interface, Chem. Phys. Lipids 33 (1983) 67–80.
[18] S.B. Hall, Z. Wang, R.H. Notter, Separation of subfractions of the hydrophobic components of calf lung surfactant, J. Lipid Res. 35 (1994) 1386–1394.
[19] A. Takahashi, T. Fujiwara, Proteolipid in bovine lung surfactant: its role in surfactant function, Biochem. Biophys. Res. Comm. 135 (1986) 527–532.
[20] O. Bizzozero, M.M. Besio, J.M. Pasquini, E.F. Soto, C.J. Gomez, Rapid purification of proteolipids from rat brain subcellular fractions by chromatography on a lipophilic dextran gel, J. Chromatog. 227 (1982) 33–44.
[21] E. Bligh, W. Dyer, A rapid method of total lipid extraction and purification, Can. J. Biochem. 37 (1959) 911–917.
[22] B.N. Ames, Assay of inorganic phosphate, total phosphate and phosphatases, Methods Enzymol. VIII (1966) 115–118.
[23] R.S. Kaplan, P.L. Pedersen, Sensitive protein assay in presence of high levels of lipid, Methods Enzymol. 172 (1989) 393–399.
[24] R.L. Searcy, L.M. Bergquist, A new color reaction for the quantitation of serum cholesterol, Clin. Chim. Acta 5 (1960) 192–199.
[25] G.L. Gaines, Insoluble Monolayers at Liquid–Gas Interfaces, Interscience Publishers, New York, 1966, pp. 73–89.
[26] P. Meller, Computer-assisted video microscopy for the investigation of monolayers on liquid and solid substrates, Rev. Sci. Instrum. 59 (1988) 2225–2231.
[27] M. Lösche, E. Sackmann, H. Möhwald, A fluorescence microscopic study concerning the phase diagram of phospholipids, Ber. Bunsenges. Phys. Chem. 87 (1983) 848–852.
[28] H.M. McConnell, L.K. Tamm, R.M. Weis, Periodic structure in lipid monolayer phase transitions, Proc. Natl. Acad. Sci. USA 81 (1984) 8249–8253.
[29] R. Peters, K. Beck, Translational diffusion in phospholipid monolayers measured by fluorescence microphotolysis, Proc. Natl. Acad. Sci. USA 80 (1983) 7183–7187.
[30] K.M. Maloney, D.W. Grainger, Phase separated anionic domains in ternary mixed lipid monolayers at the air–water interface, Chem. Phys. Lipids 65 (1993) 31–42.
[31] D.W. Grainger, A. Reichert, H. Ringsdorf, C. Salesse, An enzyme caught in action: direct imaging of hydrolytic function and domain formation of phospholipase A2 in phosphatidylcholine monolayers, FEBS Lett. 252 (1989) 73–82.
[32] H.M. McConnell, Structures and transitions in lipid monolayers at the air–water interface, Annu. Rev. Phys. Chem. 42 (1991) 171–195.
[33] R. de Koker, H.M. McConnell, Circle to dogbone: shapes and shape transitions of lipid monolayer domains, J. Phys. Chem. 97 (1993) 13419–13424.
[34] J. Israelachvili, Self-assembly in two dimensions: surface micelles and domain formation in monolayers, Langmuir 10 (1994) 3774–3781.
[35] D.J. Benvegnu, H.M. McConnell, Line tension between liquid domains in lipid monolayers, J. Phys. Chem. 96 (1992) 6820–6824.
[36] K. Nag, S.G. Taneva, J. Perez-Gil, A. Cruz, K.M. Keough, Combinations of fluorescently labeled pulmonary surfactant proteins SP-B and SP-C in phospholipid films, Biophys. J. 72 (1997) 2638–2650.

[37] S. Rivière, S. Hénon, J. Meunier, Electrostatic pressure and line tension in a Langmuir monolayer, Phys. Rev. Lett. 75 (1995) 2506–2509.

[38] S. Rivière, S. Hénon, J. Meunier, Fluctuations of a defect line of molecular-orientation in a monolayer, Phys. Rev. E 49 (1994) 1375–1382.

[39] P. Muller, F. Gallet, 1st measurement of the liquid–solid line energy in a Langmuir monolayer, Phys. Rev. Lett. 67 (1991) 1106–1109.

[40] H. Brockman, Dipole potential of lipid membranes, Chem. Phys. Lipids 73 (1994) 57–79.

[41] J.M. Smaby, H.L. Brockman, Surface dipole moments of lipids at the argon–water interface. Similarities among glycerol–ester-based lipids, Biophys. J. 58 (1990) 195–204.

[42] V. Vogel, D. Möbius, Local surface potentials and electric dipole moments of lipid monolayers: contributions of the water/lipid and the lipid/air interface, J. Colloid Interface Sci. 126 (1988) 408–420.

[43] H. Mozaffary, Cholesterol phospholipid interaction—a monolayer study, Thin Solid Films 244 (1994) 874–877.

[44] H. Mozaffary, On the sign and origin of the surface-potential of phospholipid monolayers, Chem. Phys. Lipids 59 (1991) 39–47.

[45] C.M. Jones, H.L. Brockman, Comments on the sign and origin of surface-potential of phospholipid monolayers, Chem. Phys. Lipids 60 (1992) 281–283.

[46] H. Mozaffary, Comments on the sign and origin of surface-potential of phospholipid monolayers—Reply, Chem. Phys. Lipids 60 (1992) 283–285.

[47] C. Dietrich, Z.N. Volovyk, M. Levi, N.L. Thompson, K. Jacobson, Partitioning of Thy-1, GM1, and cross-linked phospholipid analogs into lipid rafts reconstituted in supported model membrane monolayers, Proc. Natl. Acad. Sci. USA 98 (2001) 10642–10647.